Title: Competition between severing and tubulin induced repair of microtubules

Author list:

Chloe E. Shiff[1], Jane Kondev[1], Lishibanya Mohapatra[2,*]

[1]Department of Physics, Brandeis University, Waltham, MA 02454, USA

[2]School of Physics and Astronomy, College of Science, Rochester Institute of Technology, Rochester, NY 14623, USA

*** = Corresponding Author, Lead contact.**

Corresponding author email: lxmsps@rit.edu

Keywords: Severing, Tubulin-induced repair, Length control, Microtubules

Abstract:

Cytoskeletal structures aid in cell polarization, motility, and intracellular transport. Their functions are predicated on the rapid turnover of cytoskeleton proteins, which is achieved by the coordinated effort of multiple regulatory proteins whose dynamics is not well understood. Recent in-vitro experiments have investigated mixtures of regulatory proteins and cytoskeletal filaments and have reported novel synergistic effects. For example, free tubulin can repair nanoscale damages of microtubules created by proteins that sever microtubules and, in doing so, affect their disassembly. Based on this observation, we propose a model for microtubule severing as a competition between the processes of damage spreading and tubulin-induced repair. Using theory and simulations, we demonstrate that this model is in quantitative agreement with *in vitro* experiments. We predict the existence of a critical tubulin concentration above which severing becomes rare but fast. Additionally, we find that microtubule length control via severing with tubulin-induced repair is hypersensitive to changes in the concentration of free tubulin and leads to a dramatically increased dynamic range of filament lengths in steady state. Our work describes how the concerted action of multiple microtubule associated proteins produces novel dynamical properties of these cytoskeletal filaments.

Significance Statement

How cytoskeleton-associated proteins coordinate rapid turnover of cytoskeletal structures is not well understood. Recent experiments suggest that microtubule severing is the result of two competing processes of damage spreading and tubulin-induced repair. We find that this process predicts the existence of a critical tubulin concentration above which severing becomes rare but fast, and additionally, a dramatically increased dynamic range of microtubule filament lengths at steady state. This work describes how combining multiple microtubule associated proteins can produce novel dynamical properties which are not seen when these proteins are studied in isolation.

Introduction

Cells contain a cytoskeleton that aids in various cellular processes such as maintaining cell polarization, motility, and transport. The cytoskeleton is highly dynamic – it is composed of various structures that are constantly built and dismantled to assist in various functions. For example, *Chlamydomonas* use microtubule-based flagella for motility (1). Spindle fibers in the mitotic spindle shorten for chromosome separation during mitosis and meiosis.

Such changes in cytoskeletal structures requires a rapid turnover which involves an exchange of the molecular building blocks that comprise them, with the same molecules that are freely diffusing in the cytoplasm. This process does not happen in isolation but rather is facilitated by the cooperative effort of several cytoskeletal associated proteins. Remarkably, the time scales associated with the dynamics of proteins filaments in vivo are quite different from those measured in vitro. While actin networks within cells are disassembled on the order of seconds, the process takes a few minutes in vitro (2–5). Similarly, the polymerization rate of tubulin in vivo is about five to tenfold higher than in vitro at a similar concentration of pure tubulin.(6) Further, microtubules are known to switch between phases of slow growth and rapid shrinking by a process known as dynamic instability, which has been studied extensively in vitro (6). The rates of switching from shrinking to growth and vice versa (called rates of rescue and catastrophe, respectively) are believed to be modulated by several microtubule-associated proteins in vivo (7–10). Turnover rates can also be different at different stages of the cell cycle – for example, microtubule turnover rates measured in Xenopus extracts range from 3 min to 20s during interphase and mitosis, respectively(11). While much is known about the biochemical processes that facilitate the turnover of these structures in isolation, it is still not clear how different factors work together to promote filament turnover in cells.

Recently several studies have addressed this question by combining multiple factors with cytoskeletal filaments in vitro and have reported novel synergistic results that are not seen when studying each component individually. Shekhar et al. report that the cofilin-induced depolymerization rate of actin filaments increases 200-fold in the presence of cyclase associated protein/Srv-2(12). Similar studies have been done using microtubules with a recent study finding that collective effects of microtubule-associated proteins like MCAK and XMAP215 can lead to microtubule treadmilling(13). Inspired by recent experiments, we consider the interplay between the free pool of tubulin dimers and microtubule severing proteins, which fragment protein filaments(14).

A recent bioinformatic study reported that the tubulin levels in cells are autoregulated and speculated that this could be attributed to the central role tubulin plays in building microtubules (15). Efforts to understand microtubule growth have focused on the role of tubulin in the assembly of these cytoskeletal filaments, as the rate of assembly is typically proportional to the concentration of tubulin. Recently, a study summarized various ways by which the tubulin pool can affect microtubule nucleation, dynamics, and cytoskeletal organization(16). Notably, using FRET, it was shown that a local release of tubulin promoted microtubule extensions into lamellipodia, demonstrating a feedback between filament bound and soluble tubulin pools(17). Some studies have also reported that free tubulin can influence the dynamics of microtubule disassembly through interaction with proteins such as kinesin 13 (8, 18), kinesin-8 (19, 20) and severing proteins (14, 21). Severing proteins can play a key role in the reorganization of the cytoskeleton by breaking down existing structures and making more monomers available for use in new structures (22). Recent studies have found that severing proteins can seed new filament growth by releasing filaments from nucleation sites and allowing their transport within the cell (23). Katanin and spastin are well characterized examples of severing proteins for microtubule-based

structures, while cofilin and Srv-2 sever actin-based structures (21, 24–27). Katanin is thought to play two functions in mitosis and meiosis – to amplify the number of microtubules in the spindle and to uncap microtubule plus ends from the kinetochore and enable depolymerizing kinesins to target microtubules (23). Inhibition of katanin results in abnormally long mitotic spindle length in *Xenopus* extracts (28). Severing proteins play an important role in neurons as well. It has been proposed that katanin stimulates axon growth by releasing microtubules from centrosomes and severing them into shorter segments that can be transported along longer microtubules down the axon to seed new microtubule growth (29). Mutations in *Drosophila* spastin reduce dendritic arborization (branching) (30), suggesting that spastin seeds microtubule growth within newly forming regions of the dendrite. Additionally, by using in vitro systems and theory, many studies have also analyzed the effect of severing proteins on the length of cytoskeletal filaments (21, 31–35).

Thus far, most studies have focused on the effect of severing proteins in isolation, but recently experiments have examined the interplay of these proteins in presence of free tubulin. Electron microscopy images of microtubules have revealed the mechanisms by which severing proteins induce a break in the microtubule. One study reported that once severing proteins land on a microtubule, they create nanoscale damages(14). This study found that not all of the damage sites proceeded to a severing event, as free tubulin could repair the damage in some cases. Furthermore, a few in-vitro studies have reported that severing proteins enhance the rate of rescue (14, 21, 22, 34) in microtubules undergoing dynamic instability. At this point, it is unknown whether severing proteins have the same effect in vivo, where they may interact with other microtubule-associated proteins.

Inspired by these observations(14), we propose a model for microtubule severing that incorporates the newly discovered repair process by free tubulin. Using theory and simulations, we show that this new model quantitatively agrees with in vitro experimental data and makes predictions for new in vitro experiments. Significantly, we predict the existence of a critical tubulin concentration above which severing becomes rare but fast. This model also makes several implications for the dynamics of microtubules in vivo – we show that length control via severing is far more sensitive to changes in tubulin concentrations, resulting in a dramatically expanded dynamic range of filament lengths. We also report the probability distribution of lengths and the mean and coefficient of variation as a function of the various parameters of the model, which can be used to test it. In summary, our work describes how the concerted action of tubulin and severing proteins produces novel dynamical properties of microtubules that are not seen when these proteins are studied independently.

RESULTS

1. Model of microtubule severing with repair

Inspired by recent experiments(14), we consider that a microtubule severing event begins when a severing protein lands on a filament, binds to the side, and creates a damage spot (Fig. 1A). The fate of the damage created by a severing protein is determined by a competition between the removal and addition of tubulin at the damage site, eventually leading to severing or repair. We assume that monomers are added to the damage site at a rate proportional to the concentration of free tubulin $k_T[T]$ (s^{-1}) and are removed from the damage site at a rate k_r (s^{-1}), with each step either increasing or decreasing the size of damage. If the size of the damage reaches a size N_D, the filament is severed. On the other hand, if the size reaches zero, then the damage is repaired. Estimates of these model parameters are in Table 1. In this way, the size of the damage x measured in monomers (i.e. tubulin dimers) is modeled as a one-dimensional random walk with absorbing boundaries at $x = 0$ and $x = N_D$. (Fig. 1B)

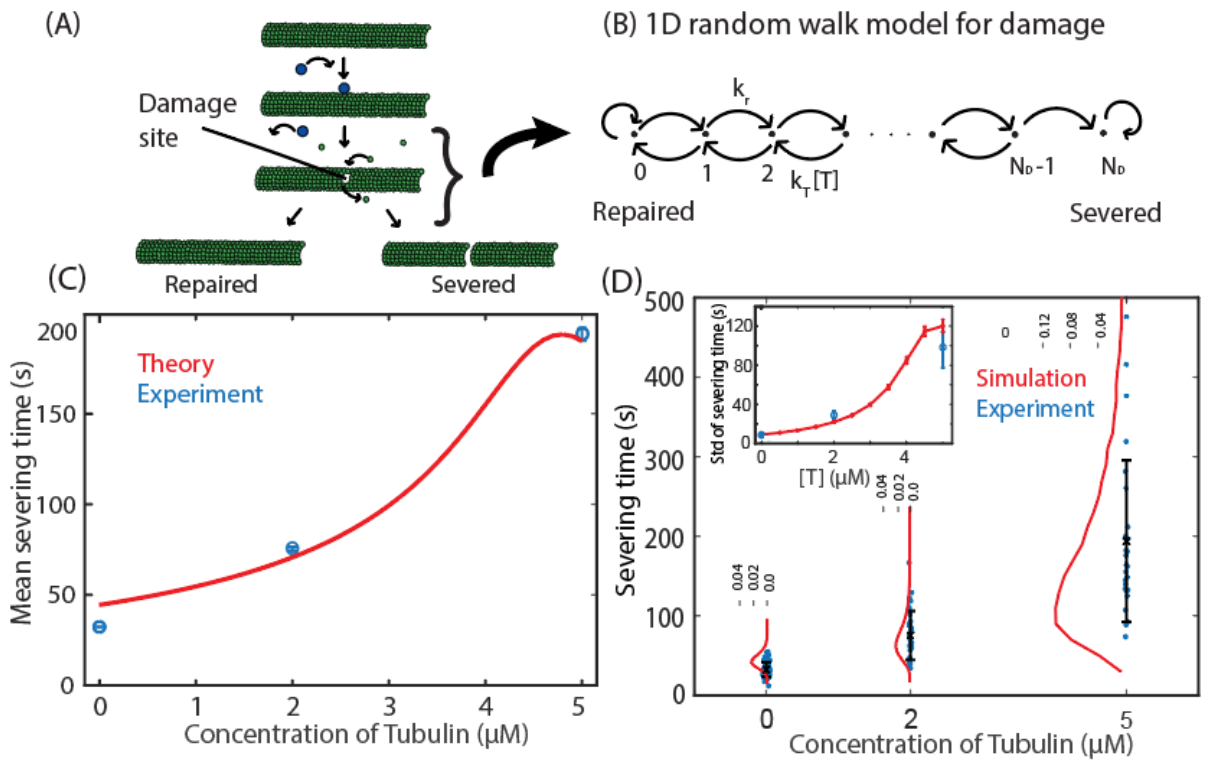

Figure 1: Microtubule severing with repair (A) Severing proteins (in blue) create small damages on microtubule lattice which either get repaired by free tubulin or lose enough monomers to sever the microtubule. (B) One-dimensional random walk model for studying the competition between removal of tubulin monomers at a rate k_r and the addition of monomers at a rate proportional to the free tubulin concentration,$k_T[T]$. (C) We use published data for the mean and the standard deviation of severing times as a function of tubulin concentration to estimate parameters of the severing model (D) The same parameters are used to compute the standard deviation (inset) and probability distribution of severing time using stochastic simulations. Comparison with published data is shown.

In this model of severing with repair, a damage site can either be repaired or progress to a severing event. Using our 1D random walk model, we find analytical expression for the probability of severing (described in section 2 and SI), and the mean time it would take to sever a filament as a function of model parameters (k_T, k_r, and N_D). Assuming an initial damage size of one monomer, and defining the ratio of tubulin addition and removal rate as a dimensionless tubulin concentration $\tilde{T} = \frac{k_T[T]}{k_r}$, we predict that the time to sever a filament has the following form ($\tilde{T} \neq 1$)

$$T_{sev}(k_T,\ k_r, N_D) = \left(\frac{\frac{1}{k_r}}{\tilde{T}-1}\right)\left(N_D\frac{(\tilde{T}^{N_D}+1)}{(\tilde{T}^{N_D}-1)} - \frac{\tilde{T}+1}{\tilde{T}-1}\right), (1)$$

In the case, $\tilde{T} = 1$. $T_{sev}(k_T,\ k_r, N_D) = \frac{1}{6k_r}(N_D^2 - 1)$. Considering $N_D \gg 1$, equation 1 has two limits. When the rate of tubulin removal is more than tubulin addition i.e.$(\tilde{T} \ll 1)$, $T_{sev}(k_T,\ k_r, N_D) \approx \frac{N_D}{k_r}(1+\tilde{T})$, i.e. severing time is linear in tubulin concentration. When $\tilde{T} \gg 1$, $T_{sev}(k_T,\ k_r, N_D) \approx \left(\frac{N_D}{k_r}\frac{1}{\tilde{T}}\right)$, i.e., severing time decreases as tubulin concentration increases. These limits indicate that

there is a critical concentration of tubulin, $[T]_c = \frac{k_r}{k_T}$, across which severing time shows different dependences on tubulin concentration. We also note that the time scale of the severing time is given by a parameter $\frac{N_D}{k_r}$. equation 1 was confirmed with stochastic simulation of the process (described in SI)

Next, we use published data to estimate a set of parameters for the model of severing with repair. We consider the plots of probability to sever and severing time as a function of tubulin concentration published in Fig. 3D and 3H in(14), and fit our model parameters (k_T, k_r, and N_D) using method of least squares, described in the SI. The sensitivity of our results on the chosen parameters is shown in Fig. S2. Using the estimated parameters, listed in Table1, we conduct stochastic simulations of the model (See section S5) to compute the distribution of severing times as a function of tubulin concentration and compare it to published data. Remarkably, just as in the data (14), we find that the distribution of severing times is asymmetric around the maximum and skewed towards large times.

The published experiment (14) suggests that severing time is monotonic in the tubulin concentration up to $5\,\mu M$. Interestingly, our model (equation 1) predicts a non-monotonic relationship between severing time and the concentration of tubulin. We find, as reported in the study, that severing time increases as the concentration of tubulin is increased but only until a certain critical concentration of tubulin. Above this concentration, as shown in equation 1, we predict that the severing time should decrease (See Fig. 2A). As we describe next, at high concentrations of tubulin, we expect that the severing events are rare (but rapid) and almost all damages are likely to quickly be repaired by the free tubulin. Note that the non-monotonicity in the severing time is a prediction of our model that can be used to experimentally test the proposed mechanism of severing by competition with repair. For example, the initial increase in the severing time was seen in experiments(14) for $[T] = 0, 2$ and $5\,\mu M$ and we predict that a concentration of tubulin larger than the critical concentration ($5\,\mu M$) will result in severing time decreasing with tubulin concentration (Fig. 2A).

2. Theoretical predictions of severing with repair

Our model makes several other predictions. The probability of severing is the probability that 1-D random walker reaches the $x = N_D$ boundary before the $x = 0$ boundary:

$$P_{sev}([T]) = \frac{\tilde{T} - 1}{\tilde{T}^{N_D} - 1} \qquad (2)$$

where we have chosen the initial damage size of 1, while N_D is the damage size that produces a severing event, and we expect, $N_D \gg 1$ (see table 1). Again, this expression has two limits (show in dotted black lines in Fig. 2): when $\tilde{T} < 1$, i.e., $[T] < [T]_c$, $P_{sev}([T]) \approx 1 - \tilde{T}$, whereas when $[T] > [T]_c$ ($\tilde{T} > 1$), $P_{sev}([T]) \approx \left(\frac{1}{\tilde{T}}\right)^{N_D - 1}$. Thus, above the critical concentration, the probability of severing is very small, and damage events that lead to a severing event, are very unlikely. We confirmed our analytical expression for the mean severing time and the probability of severing as a function of tubulin concentration by stochastic simulations (See S1).

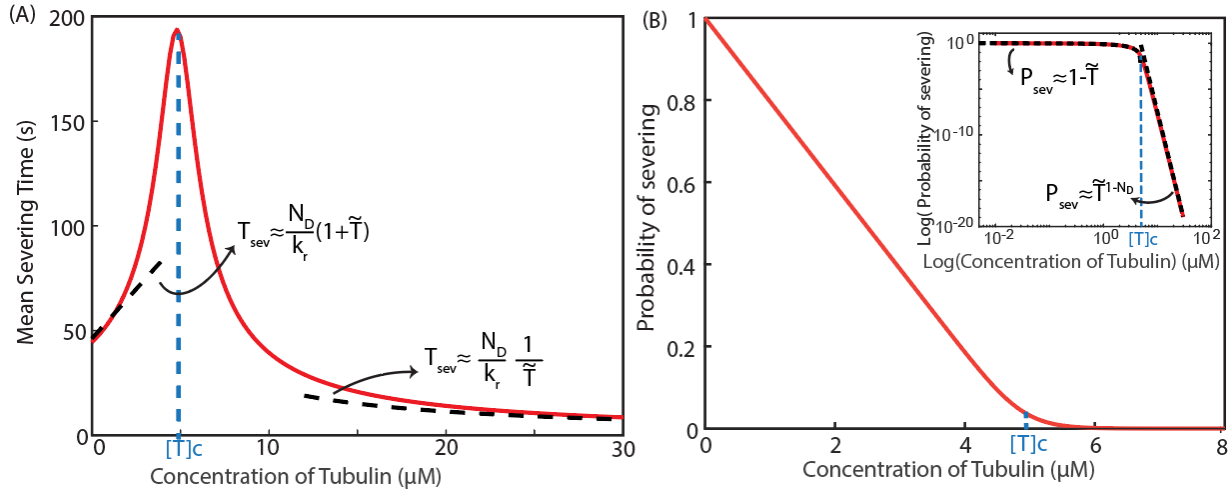

<u>Figure 2:</u> Theoretical prediction for model for microtubule severing with repair (A)The model predicts a non-monotonic relationship between severing and free tubulin concentration and predicts the existence of a critical concentration of tubulin beyond which severing time decreases. (B) Probability of severing decreases as the tubulin concentration is increased (Inset: plot in log scale).The dashed lines in both plots show the asymptotic behavior at large $[T] \gg [T]_c$ and small $[T] \ll [T]_c$ free tubulin concentrations. Parameters used to plot these graphs are listed in Table 1.

3. Length control in the presence of repair

The probability of a severing protein landing on a filament is proportional to its length. Therefore, the process of severing is a length-dependent disassembly mechanism wherein longer filaments are more likely to be severed. This results in negative feedback of filament length on filament growth and lead to control of length of cytoskeletal filaments. A number of theoretical and experimental studies (21, 28, 31, 32, 34, 35) have explored this aspect of severing. Given the recent observation of tubulin induced repair (14), we next study the implications of this repair process on the length control by severing. We consider a situation where a microtubule filament undergoes growth with a rate proportional to the free tubulin concentration and severing, where severing competes with tubulin-induced repair, as described above. Our model is simplified one where we ignore the effect of having multiple severing proteins on the microtubule at the same time. We also assume that microtubules are stabilized, and are not undergoing dynamic instability. Later in the Discussion and in the SI, we examine these assumptions and show that these do not qualitatively change our results about the mean steady-state microtubule lengths (see Fig. S3 and S4). We compare our results of the severing with repair model, to the simple severing model i.e. when there is no repair, as considered previously in (31, 34). Results of this comparison are shown in Fig. 3.

Using the scheme described in the Methods (See section S5), we conduct stochastic simulations of the filament length as a function of time and analyze the process with and without the repair or severing protein induced damage (Fig. 3). In our simulations, individual filaments grow at a rate proportional to the tubulin concentration, $k\,[\mathrm{T}]$, where k is the second order rate constant for the

tubulin binding to the end of microtubules and has the units of $(\mu M.s)^{-1}$. Severing proteins land on the side of the filament with a rate proportional to the concentration of severing proteins $[S]$ and the instantaneous length of the filament. For the simulations without the repair process, filaments get severed at a rate $k_d[S]$. In the simulation with the repair process filaments are severed at a rate proportional to the probability to sever given by equation 2, at a given concentration of tubulin, $k_d[S]P_{sev}([\mathrm{T}])$.

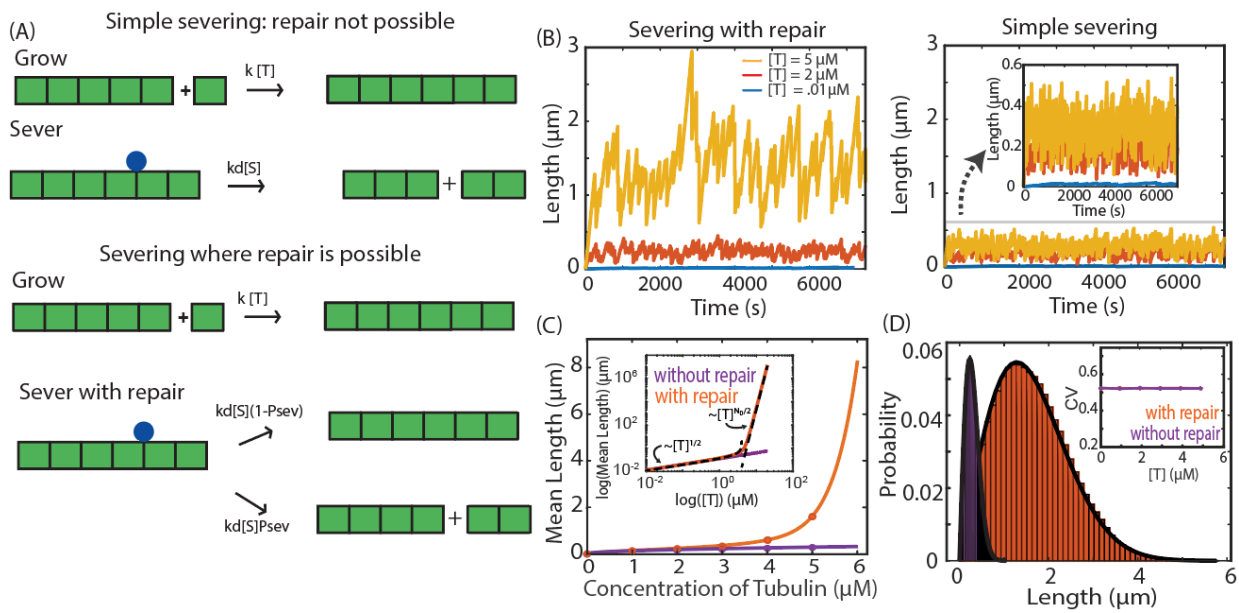

<u>Figure 3:</u> Effect of repair on filament length control via severing (A) Schematic of the two models considered. Model 1: A filament grows (with a rate $k[T]$) and is severed (with a rate $k_d[S]$). Model 2: Filament can grow (with a rate $k[T]$) and get either get severed (with rate $k_d[S]P_{sev}$) or repaired (rate $k_d[S](1-P_{sev})$) where P_{sev} (Probability of severing) was calculated using equation 1. (B) Dynamics of filament length for the two models obtained using Gillespie simulations. Dynamic range of the steady state filament lengths is bigger with repair (C) Mean steady state length as a function of tubulin concentration (Log-Log plot inset). Dots are from simulations. (D) Distribution of steady state lengths and coefficient of variation (inset) as a function of tubulin Concentration for different concentration of tubulin Parameters used for simulation are listed in Table 1.

For the two cases (simple severing and severing with repair), we generate trajectories of length over time. In both cases, we notice that, after a steep growth phase, the filament length fluctuates around a length, but the values of mean lengths obtained for each case are different. We generate trajectories at three different tubulin concentrations and observed that the mean lengths achieved by the filaments (defined as the dynamic range of filament lengths) are larger when the process of repair is included (Fig. 3B). We also analyzed this process using theory (described in Section S5 in SI) and calculated the mean filament length at steady state as $L_s^{simple\ severing} = \sqrt{\frac{\pi k[T]}{2\, k_d[\mathrm{S}]}}$,

and $L_s^{with\ repair} = \sqrt{\frac{\pi k[T]}{2\ k_d[S]P_{sev}([T])}}$. These expressions were also confirmed using simulations. As shown in Fig. 3C, while the steady state length $L_s \sim \sqrt{[T]}$ with simple severing, we observe two regimes with tubulin induced repair – when $[T] < [T]_c$, $L_s \sim \sqrt{[T]}$ and when $[T] > [T]_c$, $L_s \sim [T]^{N_D/2}$, suggesting a very high sensitivity to tubulin concentration, above the critical concentration (See SI, section S6). Note that our results for simple severing model ($L_s \sim \sqrt{[T]/[S]}$) are similar to the predictions for the "no catastrophe model" in a recently published theoretical paper which studied the effect of the severing protein spastin on the microtubules (34). In contrast, we find that including the possibility of repair of severing events in our model predicts a new regime of growth that was not described previously.

Parameters	Value used in paper	References
Concentration of Tubulin, [T]	0 - 5 μM	Vemu et al, Science 2019
Rate of replenishment, k_T	0.11 $\mu M^{-1}s^{-1}$	Estimated
Rate of removal, k_r	0.54 s^{-1}	Estimated
Minimum size of damage, x	1 monomer	Assumed
Maximum size of damage, N_D	25	Estimated
Rate of growth, k	3.4 $\mu M^{-1}\ s^{-1}$	Mickolajczyk, PNAS 2019
Concentration of severing proteins, [S]	50 nM	Vemu et al, Science 2019 (HeLa cells)
severing protein landing rate, k_d	0.002 $\mu M^{-1}\ s^{-1} nm^{-1}$	Eckert, PLOS 2012

Table 1: Parameters used in the models for the model of severing and length control with tubulin-induced repair.

We calculate analytically (described in Section S6 in SI), the probability distribution of the steady state lengths and compare our simulations with the theory in Fig. 3D. We also calculate the coefficient of variation (CV = std/mean, commonly referred to as the noise) of the steady-state mean lengths, with and without repair. Significantly, we observed that CV doesn't change with [T] (See Fig. 3D, inset and S6). This serves as a theoretical prediction for the severing process and can be used to discern this mechanism from other control mechanisms(31).

Discussion

Dynamics of protein filaments in cells (microtubules and actin filaments) are very different from what is observed in vitro (36). For example, actin networks in cells disassemble on the order of seconds whereas in vitro actin filaments disassemble over minutes (3, 4). These observations suggest that the dynamics of filament assembly are affected by proteins that associate with filaments in vivo and exert control over assembly and/or disassembly(22, 23, 37). Inspired by

recent experiments on microtubules(14), we consider one such control system and demonstrate that it leads to dynamics that are distinct from those described for microtubules in isolation.
We modeled the process of severing of microtubules as a competition between the process of removal of monomers from the damage site created by a severing protein and the repair of the damage site by binding of free monomers. We use a one-dimensional random walk model to describe this competition and compute quantities that can be measured in experiments such as the probability of severing and the time taken to successfully sever a microtubule as a function of free tubulin concentration. We quantitatively compare our theory to a number of experimental observations(14) pertaining to the effect of severing proteins on microtubules. Significantly, using our model, we predict that the time to sever has a non-monotonic dependence on tubulin concentration and reaches a maximum at a critical tubulin concentration. Next, we studied the implication of this repair process on the length of a growing filament and found that the repair process leads to an ultra-sensitivity in the lengths of microtubules as a function of tubulin concentrations.

Signatures of severing as a length-control mechanism

Often in cells, several mechanisms can be at play to control the size of a sub-cellular structure, making it challenging to distinguish between them. Key results of this paper can serve as signatures of the severing mechanism.

A key feature of length-control mechanisms is that they lead to a peaked distribution of steady-state filament lengths. Several theoretical and experimental studies have demonstrated that severing can control the length of filaments(31, 32, 34). Longer microtubules have more binding sites for severing proteins, and therefore have, a greater probability of being severed than shorter ones. This leads to negative feedback on the length of a growing microtubule and it eventually reaches a steady-state length once the disassembly rate balances the rate of assembly. The resulting distribution of steady-state lengths, in addition to being peaked, has a skewness (see Fig. 3D) which makes it distinct from other control mechanisms studied thus far (31). This skewness, predicted in theoretical studies (31, 34, 35), was observed in recent experimental studies (14, 34). Additionally, we also find that the coefficient of variation (CV) of the severing process (simple severing, severing with repair) is independent of the concentration of tubulin and has a constant value equal to 0.523 (See Fig. 3D inset and S6). Along with assuming that severing rate is small relative to growth rate, and that filaments lengths are large, this result relies on a very important assumption that the severing process is uniform across a filament and is not affected by other factors like filament aging as has been documented in the context of actin filaments, arising due to the ATP hydrolysis (32). Although a recent paper noted that the severing protein spastin severs uniformly (34) as assumed in our model, a constant CV as a function of tubulin concentration is yet another prediction that can help us test this assumption for other severing proteins.

Experimental predictions

1. *Probability of severing as a function of tubulin concentration*

We showed that a one dimensional random walk model quantitatively accounts for recent experiments of the competition between severing proteins and the free tubulin at the damage site. Using this model, we find the probability of severing decreases as the concentration of tubulin increases (See Fig. 2B). This prediction of the model can be used to further test it. Many studies have used a “severing assay” to study the effect of severing proteins on microtubules (14, 38, 39). In these experiments, severing proteins are flown into a reaction chamber with pre-formed microtubules and quantities like the number of successful severing events per unit length of the

microtubule (the severing rate) can thus be measured. Note that the maximal rate of severing is achieved when there is no free tubulin to repair the initial damage caused by a severing protein. Therefore, the ratio of the severing rate in the presence of free tubulin to the severing rate with no free tubulin is the probability of severing. At zero concentration of free tubulin, we expect all severing initiation events to be successful severing events, but that proportion would decrease as free tubulin can lead to repair, which is captured by equation 2.

2. *Non-monotonic relationship of severing time and free tubulin concentration*

Importantly, our model predicts a critical tubulin concentration $[T]_c = k_r/k_T$, where k_r is rate of removal and k_T is the rate of addition, of tubulin from the damage site. Above this critical concentration, probability of severing drops rapidly, causing the severing time to peak at $[T]_c$. By using our estimated parameters, we predict that the mean severing time should increase for 0 ≤ [T] ≤ 5μM, a prediction which agrees with results from experiments described in a recent study(14). However, at tubulin concentrations above those which were experimentally investigated in (14), $[T] > 5\ \mu M$, we find that severing time decreases. This prediction can be used to test the proposed model using the set-up described in (14).

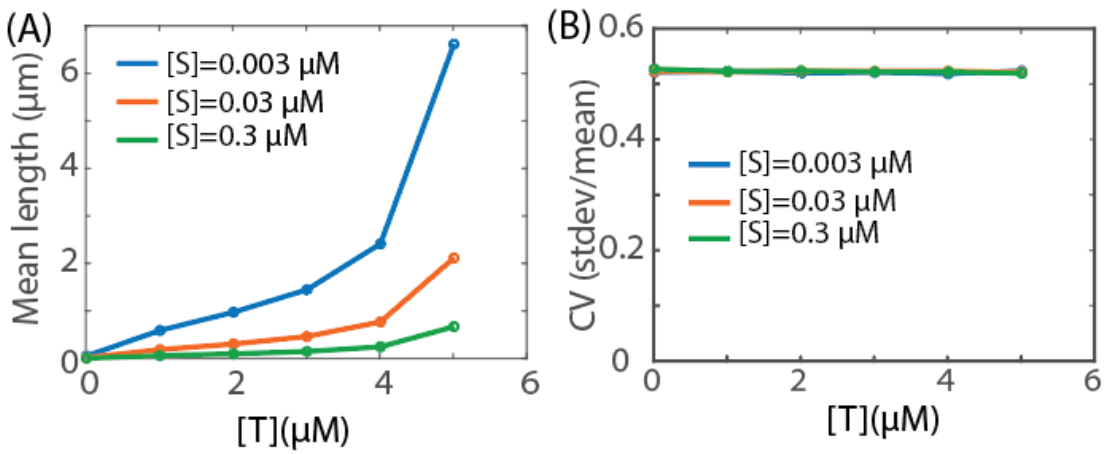

<u>Figure 4:</u> Testable prediction for model for severing with repair on filament length control (A) Mean filament length and (B) coefficient of variation at steady state as function of Tubulin concentration at different severing protein concentrations. Dynamic range is larger at lower concentration of Severing proteins, and coefficient of variation independent of tubulin and severing protein concentration. Parameters used in the simulation are listed in Table 1.

3. *Ultra-sensitivity of microtubule length control.*

Severing of filaments, which are also growing by adding monomers, leads to length control. We observe that the tubulin repair process leads to an ultra-sensitivity in the lengths of microtubules as a function of tubulin concentration (Fig. 3C, 3D).

In Fig. 4, we show results of calculations of the change in steady-state length (L_S) and the coefficient of variation as a function of two experimentally tunable knobs - tubulin and severing protein concentrations. We find a sharp increase in L_S with $[T]$ above the critical concentration $[T]_c = \frac{k_r}{k_T}$, while the coefficient of variation remains the same across all concentrations of severing proteins. These results can be tested by creating an in vitro system (14, 21, 24) in which growing

microtubules are exposed to severing proteins. We also describe the probability distribution of steady-state lengths as a function of tubulin concentrations which can be used as a more stringent test of the model (See Fig. 3D).

Examining the assumptions of the model:

In order to make the model of severing with repair analytically tractable, we made a few simplifying assumptions. Below we examine how robust our conclusions are with respect to these assumptions:

Finite severing time

In our simulations studying microtubule length-control, we ignore the time it takes for the severing event to complete once the initial damage is done, thereby assuming the possibility of multiple severing events happening at an instance on the microtubule lattice as negligible. This is a reasonable assumption at the limits of low and high tubulin concentrations, but not a valid one for intermediate tubulin concentrations.

Using the rates in Table 1, for $[T] = 0.01\mu M$, typical microtubules lengths are small (about 50 nm) and $P_{sev}[T]$ is close to 1. Time taken for a severing protein to bind to a microtubule and induce damage is $\approx \frac{1}{k_d[S]L}$ = 200s for a microtubule of length around 50 nm. In comparison, the severing time after initial damage $\approx \frac{N_D}{k_r} = 50\ secs$. Thus, at low tubulin concentrations, severing time is faster than the severing protein binding time, thus making it unlikely that multiple proteins are on the microtubule at the same time. At high tubulin concentrations $[T] > 5\ \mu M$, the microtubule filaments are about 1 micron, and the time for a severing protein to bind is around 10 secs. Although it is possible to have a large number of severing proteins on the microtubule lattice, the probability of severing is small (~ 0.025) as most damages are repaired at high concentration of Tubulin. Thus, our simplified model ignoring the possibility of multiple severing events happening simultaneously, in addition to being analytically tractable, is ideal to study the effect of severing on microtubule length control at the limits of low and high tubulin concentrations.

At intermediate tubulin concentrations (for $[T] = 2\mu M, L \sim 0.25\ \mu m$), however, the severing protein binding time is comparable to severing time (~ 50 s), making it possible that several severing events are happening at once. In order to study the implications of this scenario, we performed a full simulation wherein we tracked the locations of multiple severing proteins on a microtubule lattice. Each severing protein had a corresponding severing time, drawn from a distribution of severing times obtained from the stochastic simulation of the damage simulations (See S5 for simulation protocol). We observed that our results of large dynamic range in steady-state length from the full simulation are similar to what was seen with the simple model where we ignore the effect of having multiple severing proteins on the microtubule at the same time. Additionally, the CV vs tubulin concentration from the full simulation was identical to the one obtained from the simple model at low and high tubulin concentration. However, at intermediate values of tubulin concentrations, we observed a peak in the CV vs tubulin concentration plot (Fig. S3), which was in contrast to the constant value seen with the simple model (Fig. 3D). We also noted that this peak depended on the severing proteins concentration. This will be explored more in a future study.

Dynamic instability

Microtubules are known to switch between phases of slow growth and rapid shrinking by a process known as dynamic instability and the rates of switching from shrinking to growth and vice versa are called rates of rescue and catastrophe, respectively. In our simulations in Fig. 3 and 4, we earlier assumed that the microtubule are stabilized, and are not undergoing dynamic instability. In order to check the robustness of our results, we included dynamic instability in our simulations (see section S8 for simulation protocol) of the tubulin-induced repair on length control of microtubules and noted that it did not qualitatively change the observation of large dynamic range of filament lengths. Coincidentally, a previous theoretical study analyzed the effect of severing protein spastin on dynamic microtubules, and reported that their model predictions were similar to a model which ignored the dynamic instability ("no catastrophe" model) (34).

With stabilized microtubules, we had observed that the coefficient of variation (CV) for the steady state length fluctuations for the models of simple severing and severing with repair was a constant with respect to tubulin concentration. In contrast, when dynamic instability was included, we observed a non-monotonic relationship in CV for both models (see Fig. S4 in section S8). In our simulations, microtubule filaments grow at a rate proportional to tubulin concentration. Since severing depends on microtubule length, which is typically small at low concentrations of tubulin, dynamic instability dominates over severing in both models. In this regime, the length distributions are exponential and resulting in CV being close to 1(21, 40). However, we observe different behaviors for both models (simple severing and severing with repair) at higher tubulin concentration. In this regime, filaments grow longer and severing dominates over dynamic instability, as the number of subunits lost in a catastrophe event is small compared to the number of subunits lost due to severing. So, as expected, in the model with simple severing without dynamic instability, CV converges towards 0.523 at large concentration of tubulin. In severing with repair, we observe that CV shows a non-monotonic behavior with tubulin concentration, where it first decreases and then increases, and the dip in CV depends on the rescue rates chosen. This will be explored more in a future study. Additionally, in-vitro studies have reported an increase in rescue rates in presence of severing proteins. Several hypotheses have been proposed to explain this, such as, the incorporation of new tubulin creating a "GTP-island", which promotes rescue (14) and the accumulation of severing proteins on the tips of shrinking microtubules, where they slow shrinkage and promote rescue (21). At this point, it is unknown whether severing proteins have the same effect in vivo, where they may interact with other microtubule associated proteins.

In summary, our calculations show that tubulin and severing proteins can cause qualitatively new dynamics of microtubules. Using simulations and theory, our study describes the role of free pool of building blocks on the process of repair of damage created by severing proteins and its implications for the control of length of filaments. Here we show the existence of a critical tubulin concentration above which severing becomes strongly dependent on $[T]$, leading to a rare but fast severing. We find that microtubule length - control via severing with tubulin-induced repair is ultra-sensitive to changes in the concentrations of tubulin and the presence of repair leads to a dramatically increased dynamic range of filament lengths at steady state. Our study shows how the antagonistic action of assembly and disassembly factors can produce novel dynamical properties of microtubules.

Acknowledgements:

We wish to thank Stephanie C. Weber and Shane G. McInally for a careful reading of the manuscript, and members of Mohapatra group and Kondev group for stimulating discussions. This work was supported by the National Science Foundation through grants DMR-1610737, MRSEC DMR 2011846 (J.K., C.S.), the Simons and the HHMI foundations (J.K., L.M. and C.S) and Rochester Institute of Technology start-up funds (L.M.). We acknowledge computational support from the Brandeis HPCC which is partially supported by the NSF through DMR-MRSEC 2011846 and OAC-1920147.

References

1. L. Song, W. L. Dentler, Flagellar Protein Dynamics in Chlamydomonas. *Journal of Biological Chemistry* **276**, 29754–29763 (2001).

2. T. D. Pollard, Rate constants for the reactions of ATP- and ADP-actin with the ends of actin filaments. *J. Cell Biol.* **103**, 2747–2754 (1986).

3. N. Watanabe, T. J. Mitchison, Single-molecule speckle analysis of actin filament turnover in lamellipodia. *Science* **295**, 1083–1086 (2002).

4. T. Miyoshi, N. Watanabe, Can filament treadmilling alone account for the F-actin turnover in lamellipodia? *Cytoskeleton (Hoboken)* **70**, 179–190 (2013).

5. J. R. Kuhn, T. D. Pollard, Real-time measurements of actin filament polymerization by total internal reflection fluorescence microscopy. *Biophys J* **88**, 1387–1402 (2005).

6. A. Desai, T. J. Mitchison, Microtubule polymerization dynamics. *Annu Rev Cell Dev Biol* **13**, 83–117 (1997).

7. G. Goshima, R. Wollman, N. Stuurman, J. M. Scholey, R. D. Vale, Length control of the metaphase spindle. *Curr. Biol.* **15**, 1979–1988 (2005).

8. A. Desai, S. Verma, T. J. Mitchison, C. E. Walczak, Kin I Kinesins Are Microtubule-Destabilizing Enzymes. *Cell* **96**, 69–78 (1999).

9. R. Tournebize, *et al.*, Control of microtubule dynamics by the antagonistic activities of XMAP215 and XKCM1 in Xenopus egg extracts. *Nat Cell Biol* **2**, 13–19 (2000).

10. M. K. Gardner, M. Zanic, J. Howard, Microtubule Catastrophe and Rescue. *Curr Opin Cell Biol* **25**, 14–22 (2013).

11. A. A. Hyman, E. Karsenti, Morphogenetic Properties of Microtubules and Mitotic Spindle Assembly. *Cell* **84**, 401–410 (1996).

12. S. Shekhar, J. Chung, J. Kondev, J. Gelles, B. L. Goode, Synergy between Cyclase-associated protein and Cofilin accelerates actin filament depolymerization by two orders of magnitude. *Nat Commun* **10** (2019).

13. G. Arpağ, E. J. Lawrence, V. J. Farmer, S. L. Hall, M. Zanic, Collective effects of XMAP215, EB1, CLASP2, and MCAK lead to robust microtubule treadmilling. *Proc Natl Acad Sci U S A* **117**, 12847–12855 (2020).

14. A. Vemu, *et al.*, Severing enzymes amplify microtubule arrays through lattice GTP-tubulin incorporation. *Science* **361** (2018).

15. I. Gasic, S. A. Boswell, T. J. Mitchison, Tubulin mRNA stability is sensitive to change in microtubule dynamics caused by multiple physiological and toxic cues. *PLoS Biol* **17**, e3000225 (2019).

16. R. Ohi, C. Strothman, M. Zanic, Impact of the 'tubulin economy' on the formation and function of the microtubule cytoskeleton. *Current Opinion in Cell Biology* **68**, 81–89 (2021).

17. O. Van Geel, S. Cheung, T. W. J. Gadella, Combining optogenetics with sensitive FRET imaging to monitor local microtubule manipulations. *Scientific Reports* **10**, 6034 (2020).

18. C. E. Walczak, S. Gayek, R. Ohi, Microtubule-Depolymerizing Kinesins. *Annu. Rev. Cell Dev. Biol.* **29**, 417–441 (2013).

19. H. Arellano-Santoyo, *et al.*, A Tubulin Binding Switch Underlies Kip3/Kinesin-8 Depolymerase Activity. *Dev Cell* **42**, 37-51.e8 (2017).

20. V. Varga, C. Leduc, V. Bormuth, S. Diez, J. Howard, Kinesin-8 motors act cooperatively to mediate length-dependent microtubule depolymerization. *Cell* **138**, 1174–1183 (2009).

21. Y.-W. Kuo, O. Trottier, M. Mahamdeh, J. Howard, Spastin is a dual-function enzyme that severs microtubules and promotes their regrowth to increase the number and mass of microtubules. *Proc Natl Acad Sci U S A* **116**, 5533–5541 (2019).

22. Y.-W. Kuo, J. Howard, Cutting, Amplifying, and Aligning Microtubules with Severing Enzymes. *Trends Cell Biol* **31**, 50–61 (2021).

23. D. J. Sharp, J. L. Ross, Microtubule-severing enzymes at the cutting edge. *J Cell Sci* **125**, 2561–2569 (2012).

24. J. D. Díaz-Valencia, *et al.*, Drosophila Katanin-60 Depolymerizes and Severs at Microtubule Defects. *Biophysical Journal* **100**, 2440–2449 (2011).

25. F. Chaudhry, *et al.*, Srv2/cyclase-associated protein forms hexameric shurikens that directly catalyze actin filament severing by cofilin. *Mol. Biol. Cell* **24**, 31–41 (2013).

26. H. I. Balcer, *et al.*, Coordinated regulation of actin filament turnover by a high-molecular-weight Srv2/CAP complex, cofilin, profilin, and Aip1. *Curr. Biol.* **13**, 2159–2169 (2003).

27. A. B. Johnston, A. Collins, B. L. Goode, High-speed depolymerization at actin filament ends jointly catalysed by Twinfilin and Srv2/CAP. *Nat. Cell Biol.* **17**, 1504–1511 (2015).

28. R. Loughlin, J. D. Wilbur, F. J. McNally, F. J. Nédélec, R. Heald, Katanin Contributes to Interspecies Spindle Length Scaling in Xenopus. *Cell* **147**, 1397–1407 (2011).

29. F. J. Ahmad, W. Yu, F. J. McNally, P. W. Baas, An Essential Role for Katanin in Severing Microtubules in the Neuron. *Journal of Cell Biology* **145**, 305–315 (1999).

30. S. Jinushi-Nakao, *et al.*, Knot/Collier and Cut Control Different Aspects of Dendrite Cytoskeleton and Synergize to Define Final Arbor Shape. *Neuron* **56**, 963–978 (2007).

31. L. Mohapatra, B. L. Goode, P. Jelenkovic, R. Phillips, J. Kondev, Design Principles of Length Control of Cytoskeletal Structures. *Annu Rev Biophys* (2016).

32. J. Roland, J. Berro, A. Michelot, L. Blanchoin, J.-L. Martiel, Stochastic severing of actin filaments by actin depolymerizing factor/cofilin controls the emergence of a steady dynamical regime. *Biophys. J.* **94**, 2082–2094 (2008).

33. W. A. Elam, H. Kang, E. M. De la Cruz, Biophysics of actin filament severing by cofilin. *FEBS Lett.* **587**, 1215–1219 (2013).

34. Y.-W. Kuo, O. Trottier, J. Howard, Predicted Effects of Severing Enzymes on the Length Distribution and Total Mass of Microtubules. *Biophysical Journal* **117**, 2066–2078 (2019).

35. S. H. Tindemans, B. M. Mulder, Microtubule length distributions in the presence of protein-induced severing. *Phys. Rev. E* **81**, 031910 (2010).

36. A. J. Zwetsloot, G. Tut, A. Straube, Measuring microtubule dynamics. *Essays Biochem* **62**, 725–735 (2018).

37. M. Zanic, P. O. Widlund, A. A. Hyman, J. Howard, Synergy between XMAP215 and EB1 increases microtubule growth rates to physiological levels. *Nat Cell Biol* **15**, 688–693 (2013).

38. N. E. Ziółkowska, A. Roll-Mecak, In vitro microtubule severing assays. *Methods Mol Biol* **1046**, 323–334 (2013).

39. L. Belonogov, M. E. Bailey, M. A. Tyler, A. Kazemi, J. L. Ross, Katanin catalyzes microtubule depolymerization independently of tubulin C-terminal tails. *Cytoskeleton (Hoboken)* **76**, 254–268 (2019).

40. M. Dogterom, S. Leibler, Physical aspects of the growth and regulation of microtubule structures. *Phys. Rev. Lett.* **70**, 1347–1350 (1993).